Limnol. Oceanogr., 47(4), 2002, 997–1011

Phytoplankton iron limitation in the Humboldt Current and Peru Upwelling

D. A. Hutchins,[1] *C. E. Hare, R. S. Weaver, Y. Zhang, and G. F. Firme*
College of Marine Studies, University of Delaware, 700 Pilottown Road, Lewes, Delaware 19958

G. R. DiTullio, M. B. Alm, S. F. Riseman, J. M. Maucher, and M. E. Geesey
Grice Marine Laboratory, University of Charleston, Charleston, South Carolina 29412

C. G. Trick
Department of Plant Sciences, University of Western Ontario, London, Ontario N6A 5B7, Canada

G. J. Smith, E. L. Rue, J. Conn, and K. W. Bruland
Institute of Marine Sciences, University of California, Santa Cruz, Santa Cruz, California 95064

Abstract

We investigated phytoplankton Fe limitation using shipboard incubation experiments in the high-nutrient South American eastern boundary current regime. Low ambient Fe concentrations (~0.1 nM) in water collected from the Humboldt and Peru Currents were supplemented with a range of added Fe levels up to 2.5 nM. Phytoplankton chlorophyll *a*, photosystem II photosynthetic efficiency, and nitrate and phosphate drawdown increased in proportion to the amount of Fe added. The Humboldt Current algal community after Fe additions included colonial and flagellated *Phaeocystis globosa* and large pennate diatoms, whereas the Peru Upwelling assemblage was dominated by coccolithophorids and small pennate diatoms. Apparent half-saturation constants for growth of the two communities were 0.17 nM Fe (Humboldt Current) and 0.26 nM Fe (Peru Upwelling). Net molar dissolved $Si(OH)_4$: NO_3^- drawdown ratios were low in both experiments (~0.2–0.7), but net particulate silica to nitrogen production ratios were higher. Fe limitation decreased net $NO_3^- : PO_4^{3-}$ utilization ratios in the Humboldt Current incubation to well below Redfield values. Phytoplankton community sinking rates were decreased by Fe additions in the Peru Upwelling, suggesting potential Fe effects on carbon export. Our results confirm that primary producers in the Peru Upwelling/Humboldt Current system can be limited by Fe, but the biological and biogeochemical consequences of Fe limitation differ from Fe-limited California coastal upwelling waters that have been previously studied.

The first evidence for phytoplankton Fe limitation was from shipboard growout experiments in the subarctic Pacific, the equatorial Pacific, and the Southern Ocean (de Baar et al. 1990; Martin et al. 1991). These results were later confirmed by mesoscale open ocean Fe fertilization experiments in two of these oceanic high-nutrient, low-chlorophyll (HNLC) areas (Martin et al. 1994; Coale et al. 1996a; Boyd et al. 2000). The isolation of these regions from terrestrial Fe sources and the scarcity of Fe relative to major nutrients in upwelled water play a key role in maintaining the HNLC condition. The biogeochemical effects of Fe limitation are, however, not limited only to these three HNLC regimes. Fe availability limits growth or photosynthetic efficiency of diatoms (DiTullio et al. 1993), as well as cyanobacteria such as *Trichodesmium* (Rueter et al. 1992) and *Synechococcus* (Behrenfeld and Falkowski 1999) in the oligotrophic central gyres.

The most recent additions to the list of Fe-limited regimes are coastal upwelling areas. These small areas along the western coasts of the Americas and Africa cover only ~0.5–1% of the ocean's surface, but support about 11% of total global new production, totaling 0.8 Pg C yr^{-1}. This new production is more than that estimated for all of the subtropical gyres combined (0.5 Pg C yr^{-1}) and is equivalent to about 73% of the annual new production over the entire Southern Ocean (1.1 Pg C yr^{-1}, Chavez and Toggweiler 1995). The importance of coastal upwelling areas in the carbon cycle is also shown by estimates that organic carbon burial rates are an order of magnitude higher ($0.3–0.6 \times 10^8$ tons yr^{-1}) than in all oceanic upwelling areas combined ($0.03–0.09 \times 10^8$ tons yr^{-1}, Brink et al. 1995). Because of their short, productive food chains and ease of accessibility, they also provide much of the biological resources that humans harvest from the sea (Ryther 1969).

In parts of the California coastal upwelling system, Fe addition allows nitrate drawdown and produces blooms of large, heavily silicified chain-forming diatoms such as *Chaetoceros* (Hutchins et al. 1998; Bruland et al. 2001). Fe availability also regulates major nutrient biogeochemistry in this region. Silicic acid to nitrate (Si : N) molar utilization ratios in low-Fe coastal California waters are 2–3, but fall to a nutrient-replete diatom ratio of ~1 (Brzezinski 1985) when Fe is supplied (Hutchins and Bruland 1998; Firme et al. in press). There are only minimal riverine inputs along most of the California coast during the summer upwelling season, so

[1] Corresponding author (dahutch@udel.edu).

Acknowledgments

We thank the captain and crew of the R/V *Melville* and the governments of Ecuador and Peru. Support was provided by NSF OCE 9811062 (D.A.H.), OCE 9811114 and CEBIC (K.W.B.), OCE 9907931 (G.R.D.), and CEBIC (C.G.T.).

the primary source of Fe to the euphotic zone is the interaction of upwelled water with shallow shelf sediments (Johnson et al. 1999; Bruland et al. 2001). The continental shelf along much of California is very narrow, and it is in these areas that phytoplankton Fe limitation is most severe.

Fe limitation is likely to occur in other coastal regimes as well when high upwelled major nutrient fluxes are combined with low Fe inputs from rivers and continental shelf sediments. In particular, the world's largest and most productive coastal upwelling system off the coast of Peru and Chile meets these criteria. This area is bordered by the Atacama Desert, so riverine inputs are negligible. Like California, the continental shelf along much of Peru is very narrow, which should greatly reduce the supply of sedimentary Fe to phytoplankton communities. This hypothesis is indirectly supported by prior observations of conditions off western South America, such as sporadic HNLC conditions and silicic acid depletion relative to nitrate (Minas and Minas 1992; Dugdale et al. 1995), which we now know to be diagnostic of Fe limitation in California waters.

We report here on two shipboard Fe addition experiments, one carried out in the Peru Current upwelling region and one in the offshore northern Humboldt (Peru/Chile) Current, a transitional zone between the coastal upwelling and the oceanic equatorial Pacific HNLC area. We examined the effects of adding a range of Fe concentrations on nutrient biogeochemistry, phytoplankton growth, and taxonomic composition. The results of these experiments allowed us to compare the biological and biogeochemical consequences of Fe limitation off Peru with the results of previous investigations in the California coastal HNLC area.

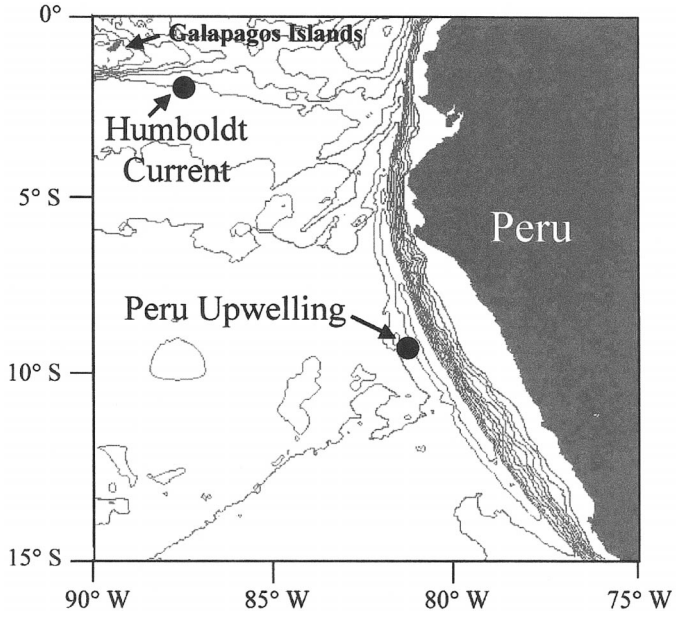

Fig. 1. Stations where near-surface water was collected for the Humboldt Current and Peru Upwelling Fe addition experiments, with bathymetry shown to illustrate proximity to shelf sources of Fe.

Methods

Water collections and shipboard incubations—Shipboard Fe addition experiments began with the collection of phytoplankton communities on 7 September 2000 from the Humboldt Current (2°17.5′S, 87°30.7′W) and on 15 September 2000 from northern Peruvian coastal waters (9°39.0′S, 81°23.3′W) (Fig. 1). Sea surface temperatures and salinities at these locations were 20.2°C and 34.53 (Humboldt Current) and 18.3°C and 35.13 (Peru Current), respectively. Water was collected from 8–10 m deep using a trace metal–clean Teflon pump system and was dispensed into acid-washed 2.7-liter polycarbonate bottles for 4- or 5-day deckboard incubations at ~40% of ambient light level, as described in Hutchins et al. (1998). Experiments used triplicate unamended controls and triplicate bottles supplemented with Fe additions ($FeCl_3$ in 0.01 N HCl) of 0.1, 0.5, and 2.5 nM (Humboldt Current) and 0.2, 0.4, 0.8, and 2.5 nM (Peru Upwelling).

Dissolved and particulate nutrients and Fe—Dissolved nutrients (nitrate + nitrite, phosphate, and silicic acid) were analyzed daily at sea on 0.2-μm filtered samples using a Lachat Quick Chem autoanalyzer. Particulate organic carbon (POC) and nitrogen (PON) were measured in the lab using CHN analyses of GF/F-filtered samples (Hutchins et al. 1998), and biogenic silica (BSi) analyses were performed on 0.6-μm filtered samples according to Brzezinski and Nelson (1995). Electrochemical total dissolved Fe measurements were made at sea using cathodic stripping voltammetry on 0.2-μm filtered, ultraviolet (UV)-oxidized seawater samples (Rue and Bruland 1997). Total dissolved Fe concentrations at both stations were extremely low at ~0.1 nM (Humboldt Current) and ~0.08 nM (Peru Upwelling).

Phytoplankton parameters—In all incubation experiments, daily fast repetition rate fluorometry analyses (FRRF, Behrenfeld and Falkowski 1999) were used to estimate Fe effects on photosynthetic efficiency (F_v/F_m) and photosystem II cross-sectional areas (σ_{PSII}). Samples were dark-adapted for 30 min and analyses were performed at the same time of day to prevent diel periodicity bias. Chlorophyll *a* (Chl *a*) size distributions were monitored daily using Whatman GF/F (total Chl *a*) and 5.0-μm polycarbonate filters (>5.0 μm) in acetone extracts using the nonacidified fluorometric technique (Welschmeyer 1994). Live flow cytometry samples were analyzed within 1 h of sampling using a Becton Dickinson FACSCalibur flow cytometer (15 mW argon ion laser, 488 nm excitation) to count large, strongly red autofluorescent phytoplankton (e.g., diatoms), smaller red autofluorescent nanoplankton (e.g., eukaryotic flagellates), and orange and red autofluorescent picophytoplankton (e.g., *Synechococcus* and *Prochlorococcus,* respectively) (Durand and Olson 1996). Epifluorescence microscopy cell counts were carried out on final samples from the experiments using 50-ml glutaraldehyde-preserved samples (Hutchins et al. 1998, 2001). Phytoplankton abundance in initial samples was found to be too low to obtain reliable visual counts. In the Peru Upwelling study only, we used the SETCOL method (Bienfang 1981) to measure phytoplankton community sinking rates at the end of the 5-d incubations.

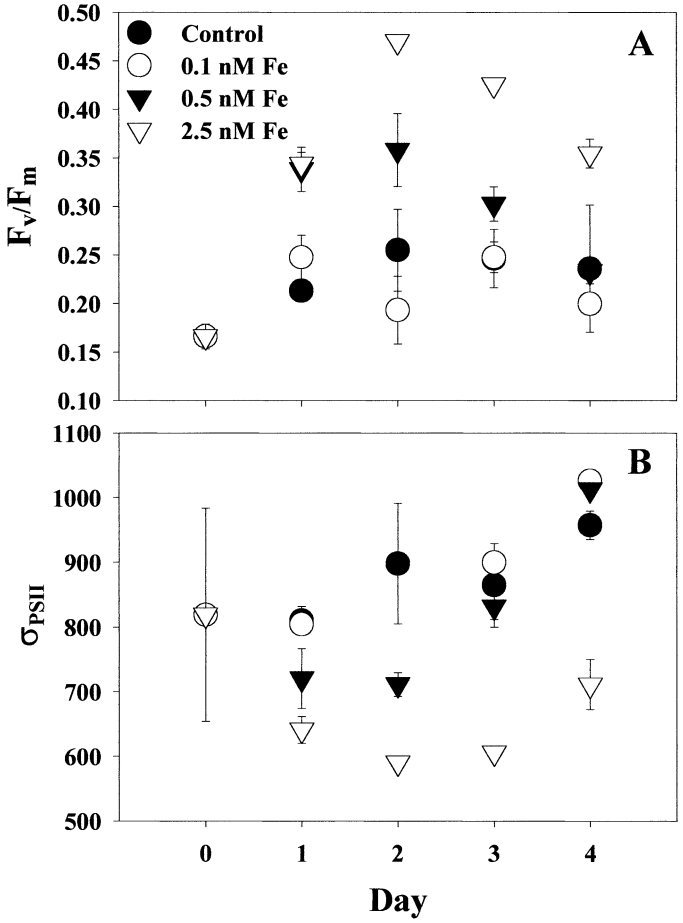

Fig. 2. Photosynthetic parameters in the 4-d Humboldt Current incubations measured with fast repetition rate fluorometry (FRRF). (A) Photosynthetic efficiency assessed as variable over maximum fluorescence, F_v/F_m. (B) The cross-sectional area of photosystem II, σ_{PSII}. Symbols and error bars represent the means and standard deviations of measurements on triplicate bottles. Controls, closed circles; 0.1-nM Fe additions, open circles; 0.5-nM Fe additions, closed triangles; 2.5-nM Fe additions, open triangles.

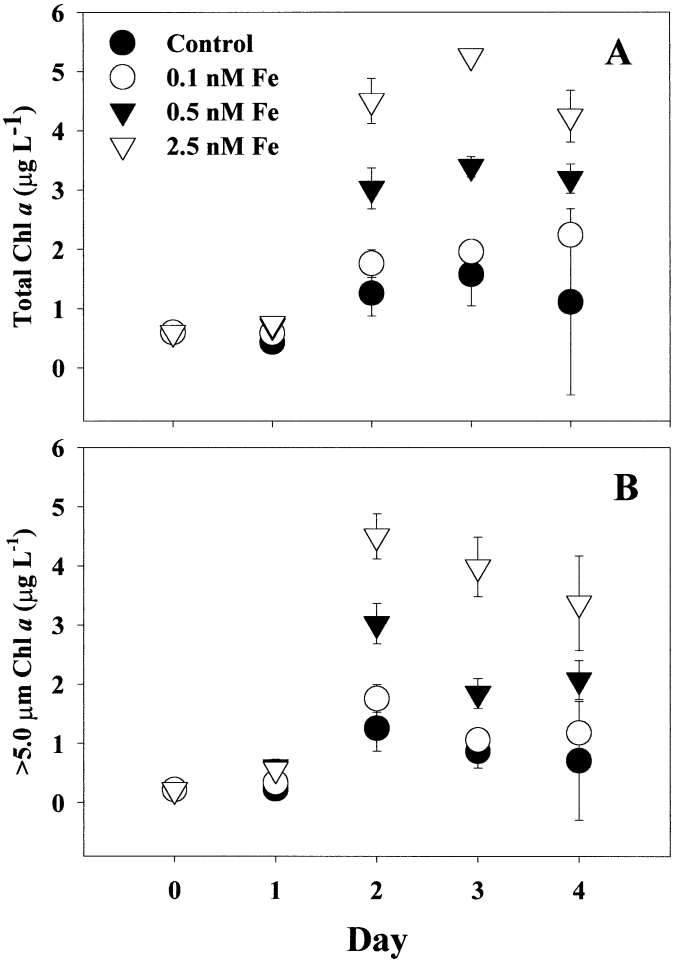

Fig. 3. Fluorometrically determined Chl *a* concentrations in the Humboldt Current incubations. (A) Total Chl *a*; (B) >5 μm Chl *a*. Symbols and error bars are as in Fig. 2.

Taxon-specific phytoplankton accessory pigments were measured using high-performance liquid chromatography (HPLC) to estimate the abundance of major phytoplankton groups (DiTullio et al. 1993, in press). Because of the large sample volume required (1–2 liters), pigments were measured only in the initial and final incubation samples. Samples were filtered (Whatman GF/F) and frozen in liquid nitrogen until analysis. Pigment concentration data were analyzed using the ChemTax program (Mackey et al. 1996) to estimate the abundance of specific taxonomic groups of algae relative to the total Chl *a* present. Details of the initial pigment ratios used in the ChemTax analysis will be presented elsewhere.

Results

Humboldt Current—Phytoplankton response: The response of phytoplankton photosynthetic efficiency (F_v/F_m) was directly related to the amount of added Fe (Fig. 2A). F_v/F_m in initial samples was low (0.17) but doubled by the first day in both 0.5- and 2.5-nM treatments and continued to increase to a maximum of 0.47 on day 2 in the 2.5-nM bottles. Day 1 values in the control and 0.1-nM Fe addition were 0.21 and 0.25, respectively, and F_v/F_m in these two treatments was low throughout the incubation. F_v/F_m in the two highest Fe addition treatments decreased on days 3 and 4, perhaps indicating the onset of nutrient or Fe limitation resulting from increased biomass.

The functional σ_{PSII} (Falkowski and Kolber 1995) showed an inverse dependence on added Fe levels and was nearly a mirror image of the pattern observed for F_v/F_m (Fig. 2B). σ_{PSII} decreased rapidly over the first 2 d at the two highest Fe levels then increased again as F_v/F_m decreased at the end of these incubations. In contrast, σ_{PSII} was relatively constant in the control and 0.1-nM Fe addition bottles for the first 3 d of the experiment, followed by a small increase on day 4.

Fluorometrically determined, size-fractionated Chl *a* showed a strong dependence on the amount of added Fe (Fig. 3). Although total Chl *a* in the controls approximately doubled over the 4-d incubation (Fig. 3A), total Chl *a* increases in the 0.1-nM Fe addition were larger. Incrementally

greater increases were observed in the 0.5- and 2.5-nM Fe addition. The lag period before exponential growth occurred was only 1 d, shorter than in many previous growout experiments from other regions (de Baar et al. 1990; Boyd et al. 1996; Hutchins et al. 2001). Initially, about a third of the total Chl *a* was in the large size class (>5 μm, Fig. 3B). Throughout the incubations, Chl *a* increases were dominated by the large size class, which accounted for one-half to three-quarters of the total Chl *a* at the final timepoint.

Initially, the water had low concentrations of all taxon-specific accessory pigments except Chl c_3 (Table 1). ChemTax analysis (Table 2) indicated that the sample was initially dominated by haptophytes. A 19′-hexanoyloxyfucoxanthin (19-hex) to fucoxanthin ratio of 1.6 confirmed the dominance of Type 4 haptophytes such as *Phaeocystis*. The small amount of fucoxanthin indicated that diatoms were a minor component of the initial sample, as were divinyl Chl *a*–containing prochlorophytes. Somewhat larger concentrations of Chl *b* and alloxanthin indicated the presence of prasinophytes and cryptophytes, respectively. Concentrations of zeaxanthin (primarily found in cyanobacteria) and peridinin (dinoflagellates) were low. Only a minor fraction of the total Chl *a* was present as chlorophyll degradation products (phaeophytins *a* and *b* and phaeophorbide, Table 1).

The increases in HPLC-determined Chl *a* concentrations during the incubations were similar to those observed by fluorometry. Concentrations of divinyl Chl *a*, Chl *b*, peridinin, and zeaxanthin decreased from the initial values (Table 1). Chl c_3 decreased in the controls, but final concentrations in +Fe bottles were 4–10× those in controls. Fucoxanthin increases were large in Fe-amended bottles and were similar in magnitude to the increases seen in Chl *a*; 19′-butanoyloxyfucoxanthin (19-but) nearly doubled in all +Fe treatments and controls, and 19-hex increased to 2–4× the initial concentrations, with the largest increases in the two highest Fe treatments. In the control and 0.1-nM Fe treatment, alloxanthin increased to more than triple the initial concentration, and in the 0.5- and 2.5-nM Fe treatments it increased >5×. In general, there was a moderate increase in algae that contain Chl c_3 and 19-hex (pelagophytes and haptophytes) and a large increase in algae that contain fucoxanthin only (diatoms) or alloxanthin (cryptophytes).

ChemTax pigment data analysis indicated that phytoplankton taxonomic composition in all treatments and controls shifted from that initially observed. Although there were biomass differences between treatments, the relative algal composition was similar between treatments (Table 2). Diatom abundance increased dramatically until they were codominant with type 4 haptophytes in all treatments. Cryptophytes were of tertiary importance in these treatments.

Type 3 haptophytes (e.g., *Emiliania huxleyi*), pelagophytes, prasinophytes, and cyanobacteria were of minor abundance in every treatment, never containing more than a small fraction of the total Chl *a* (Table 2). Prochlorophytes and dinoflagellates disappeared from the incubations. As a percentage of total Chl *a*, phaeopigments increased from the initial value of 16% to 41–46% in the control and the two lower Fe addition treatments and to 25% in the high-Fe treatment (data not shown).

Flow cytometry data indicated that cyanobacteria (*Syne-*

Table 1. Taxon-specific phytoplankton pigment and phaeopigment concentrations (ng L^{-1}) at the initial timepoint and at the end of the incubations. Values are the means and errors are the standard deviations of measurements from duplicate (Humboldt Current) or triplicate (Peru Upwelling) bottles.

	Humboldt Current						Peru Upwelling					
			Fe addition (nM), final						Fe addition (nM), final			
	Initial	Control final	0.1	0.5	2.5		Initial	Control final	0.2	0.4	0.8	2.5
Divinyl Chl *a*	29 ± 1	0	0	0	0		14 ± 1	0	0	0	0	0
Zeaxanthin	29 ± 1	21 ± 3	22 ± 3	16 ± 22	38 ± 7		59 ± 5	59 ± 21	96 ± 9	136 ± 17	140 ± 32	165 ± 35
Chl c_3	1,274 ± 36	155 ± 14	731 ± 34	1,184 ± 114	1,513 ± 99		306 ± 20	245 ± 49	538 ± 70	549 ± 15	575 ± 100	599 ± 39
Fucoxanthin	83 ± 7	348 ± 14	473 ± 53	613 ± 28	745 ± 63		157 ± 7	392 ± 6	1,762 ± 536	2,240 ± 590	2,067 ± 151	2,060 ± 286
19-hex	131 ± 3	334 ± 11	234 ± 315	484 ± 51	486 ± 7		713 ± 47	340 ± 65	796 ± 106	684 ± 34	567 ± 155	513 ± 146
19-but	48 ± 5	83 ± 3	90 ± 0	91 ± 17	93 ± 7		65 ± 3	153 ± 49	341 ± 7	306 ± 33	220 ± 26	213 ± 38
Chl *b*	97 ± 5	37 ± 3	53 ± 0	75 ± 25	52 ± 8		95 ± 1	38 ± 9	71 ± 11	85 ± 14	78 ± 24	96 ± 19
Alloxanthin	15 ± 0	50 ± 5	52 ± 7	80 ± 19	81 ± 10		94 ± 27	61 ± 21	93 ± 71	180 ± 58	161 ± 52	182 ± 80
Perdinin	11 ± 10	0	0	0	0		30 ± 21	0	0	0	36 ± 31	49 ± 20
Phaeophytin *b*	6 ± 0	152 ± 9	238 ± 33	284 ± 43	225 ± 15		97 ± 6	74 ± 14	128 ± 11	102 ± 42	103 ± 21	98 ± 14
Phaeophytin *a*	54 ± 2	124 ± 11	152 ± 24	189 ± 20	264 ± 32		137 ± 3	163 ± 34	801 ± 244	962 ± 58	966 ± 64	1,028 ± 103
Phaeophorbide	21 ± 4	237 ± 13	338 ± 75	341 ± 43	180 ± 52		29 ± 6	699 ± 317	1,068 ± 104	983 ± 267	940 ± 132	1,329 ± 289

Table 2. Phytoplankton assemblage composition based on ChemTax results at the initial timepoint and at the end of the incubations. Values give the total Chl *a* content (μg L^{-1}) in the sample and the percentage of total Chl *a* in each algal group in the sample. For prochlorophytes, the value is for divinyl Chl *a*.

	Humboldt Current					Peru Upwelling					
		Control	Fe addition (nM), final				Control	Fe addition (nM), final			
	Initial	final	0.1	0.5	2.5	Initial	final	0.2	0.4	0.8	2.5
Total Chl *a* (μg L^{-1})	0.5	1.2	1.6	2.0	2.7	1.1	1.1	3.9	4.7	4.5	4.8
Percentage of total Chl *a* in each algal group											
Diatoms	8	27	30	30	37	0	30	55	58	57	56
Dinoflagellates	3	0	0	0	0	2	0	0	0	1	2
Cryptophytes	16	24	19	23	21	22	18	9	13	12	13
Pelagophytes	1	4	2	1	2	3	16	11	10	9	8
Type 3 Haptophytes	10	10	3	2	7	38	19	15	10	7	6
Type 4 Haptophytes	28	28	39	38	27	17	0	1	0	4	4
Prasinophytes	18	3	3	3	3	6	4	2	2	2	2
Chlorophytes	0	0	0	1	0	0	0	0	0	0	0
Cyanobacteria	4	4	3	2	4	10	12	6	7	7	8
Prochlorophytes	6	0	0	0	0	1	0	0	0	0	0

chococcus and *Prochlorococcus*) were numerically dominant in the initial collected water, although their actual abundance was relatively low (~3,800 cells ml^{-1}), and they did not contain a major fraction of the total Chl *a* (Table 2). Cyanobacteria peaked on day 2 of the experiments and then declined to slightly below initial levels, and Fe additions had little or no apparent effect on their abundance (Fig. 4A). The abundance of eukaryotic nanoplankton also showed no clear response to the Fe additions and remained relatively constant (400–600 cells ml^{-1}) throughout the incubation (Fig. 4B). After an initial lag period, larger eukaryotic phytoplankton were much more abundant at the end of the experiment in the three Fe addition treatments than in the control (Fig. 4C).

Microscopic cell counts from the end of the incubation show that cell numbers of all diatoms in the +Fe incubations were roughly 3–4× higher than in controls (Table 3). Counts in all treatments were dominated by small unicellular pennate diatoms, especially several species of *Navicula* and *Pseudo-nitzschia*. However, numerically rarer but larger species of chain-forming pennate diatoms (*Nitzschia* spp.) likely contributed a substantial share of total diatom biomass in the Fe addition treatments. The abundance of large unicellular centric diatoms (Coscinodiscaceae) increased dramatically with increasing Fe availability, especially in the 2.5-nM Fe addition (12× the controls). Likewise, the large diatom genera *Guinardia* and *Rhizosolenia* were only observed in the samples amended with 0.5- and 2.5-nM Fe, and *Chaetoceros* was seen only in the latter treatment.

Numbers of individual flagellated *Phaeocystis globosa* cells showed no strong trend among treatments (Table 3). However +Fe bottles were visibly dominated at the end of the incubation by numerous macroscopic *P. globosa* colonies, whereas few were observed in the controls. Colonies were also occasionally observed in the preserved microscopy samples, but only in the bottles amended with 0.5 or 2.5 nM Fe. Because of the difficulty in quantifying cell numbers in *P. globosa* colonies, colony counts are not presented. As a result, the *P. globosa* cell numbers reported undoubtedly represent an underestimate of the true contribution from this group. Dinoflagellates were present in low abundance and were highly variable among replicates (*see* SDs, Table 3), as were cyanobacteria. Surprisingly in light of the pigment and flow cytometry results, nanoflagellates (other than *P. globosa*) were not observed in the microscopy samples, although preservation of small cells (including cyanobacteria) was relatively poor in this experiment, similar to other studies (e.g., Gieskes and Kraay 1983).

Nutrient biogeochemistry: Nitrate in control bottles declined by only 16% over the 4-d incubation (Fig. 5A; Table 4). In contrast, nitrate was nearly depleted by the third day in the highest Fe addition (2.5 nM), and by the fourth day in the 0.5 nM Fe treatment. The lowest Fe addition (0.1 nM) used about two-thirds of the initial nitrate by the end of the experiment.

Phosphate utilization was similar to that of nitrate, with amounts used ranging from one-quarter (controls) to two-thirds (2.5-nM Fe addition) of the initial concentration (Fig. 5B; Table 4). Compared to nitrate and phosphate, Fe additions had much less effect on silicic acid drawdown in this experiment (Fig. 5C; Table 4). The controls and 0.1-nM Fe treatments consumed about a third of the original 6.6 μM $Si(OH)_4$, and the two higher Fe additions used about half.

Net community $Si(OH)_4 : NO_3^-$ utilization ratios in the Humboldt Current experiment were 2–3× higher in controls than in any of the Fe addition bottles (Table 4). Notable however were the low absolute dissolved Si : N drawdown ratios in all incubations (0.71, controls; ~0.2–0.3, +Fe bottles) in this regime in comparison to previous results from California (2–3, controls; ~1, +Fe treatments, Hutchins et al. 1998). Fe also appeared to have a major effect on NO_3^- : PO_4^{3-} utilization ratios in this tropical Pacific experiment. Although final N : P utilization ratios were at or above Redfield values in all three +Fe treatments (~16–20), Fe limitation in the controls resulted in a much lower value (~9).

POC and PON production increased with added Fe. Bio-

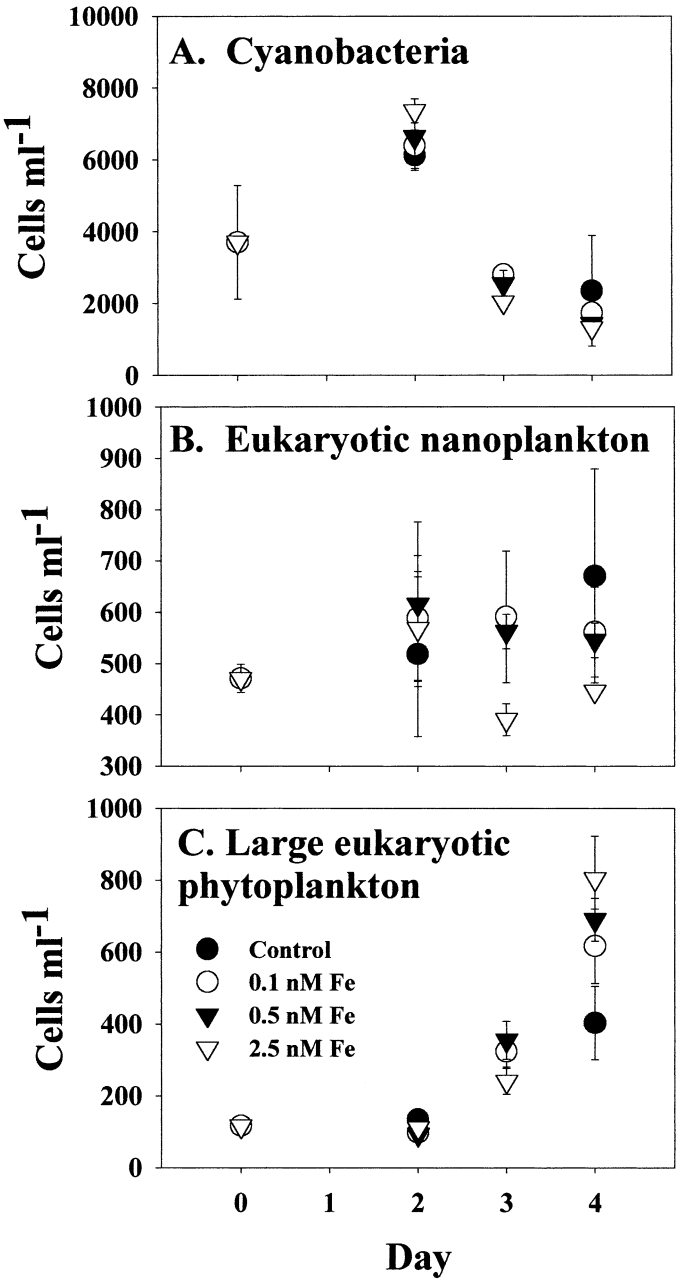

Fig. 4. Results of flow cytometry analyses of phytoplankton abundance during the Humboldt Current experiment. (A) Cyanobacteria. (B) Eukaryotic nanoplankton. (C) Large eukaryotic phytoplankton, chiefly diatoms. Symbols and error bars are as in Fig. 2.

genic silica (BSi) production, however, was approximately equal in all of the treatments (Table 4). Net BSi : POC and BSi : PON production ratios and nitrate : silicate drawdown ratios suggested that the phytoplankton biomass produced in controls was considerably more silicified than in the +Fe bottles. Except for the 2.5-nM treatment, though, BSi : PON production ratios were substantially higher (1.1–2.2×) than the values calculated from dissolved N and Si drawdown.

Peru Upwelling—Phytoplankton response: The responses of F_v/F_m and σ_{PSII} (Fig. 6A,B) and fluorometrically deter-

Table 3. Microscopic cell counts (cells ml^{-1}) from the final day of the Humboldt Current (day 5) and Peru Upwelling (day 4) Fe addition experiments. Errors are the standard deviations of triplicate bottles. no, not observed.

	Humboldt Current					Peru Upwelling					
		Fe addition (nM)					Fe addition (nM)				
	Control	0.1	0.5	2.5	Control	0.2	0.4	0.8	2.5
Total diatoms	407 ± 312	1,345 ± 320	1,068 ± 262	1,791 ± 362	2,340 ± 1,180	10,660 ± 7,280	16,180 ± 3,300	12,220 ± 1,040	61,200 ± 8,240
Pennates	400 ± 312	1,328 ± 326	1,040 ± 256	1,670 ± 340	2,340 ± 1,180	10,660 ± 7,280	16,180 ± 3,300	12,220 ± 1,040	61,200 ± 8,240
Coscinodiscacea	7 ± 7	17 ± 6	18 ± 9	83 ± 10	no	no	no	no	no
Chaetoceros	no	no	no	24 ± 2	no	no	no	no	no
Guinardia	no	no	8 ± 8	8 ± 8	no	no	no	no	no
Rhizosolenia	no	no	2 ± 0	6 ± 1	no	no	no	no	no
Phaeocystis (unicellular)	646 ± 270	144 ± 49	748 ± 552	540 ± 388	3,840 ± 270	10,740 ± 2,880	8,280 ± 1,870	3,960 ± 3,220	10,660 ± 1,230
Nanoflagellates	no	no	no	no	7,880 ± 330	16,080 ± 2,480	9,560 ± 12,550	16,340 ± 6,480	17,340 ± 130
Dinoflagellates	28 ± 37	21 ± 5	37 ± 16	16 ± 16	no	3,120 ± 2,500	3,000 ± 2,800	2,360 ± 2,000	7,180 ± 9,800
Cyanobacteria	330 ± 90	1,348 ± 626	916 ± 804	1,086 ± 1,882	19,620 ± 2,900	25,200 ± 10,360	41,000 ± 6,640	22,200 ± 13,420	39,000 ± 28,600

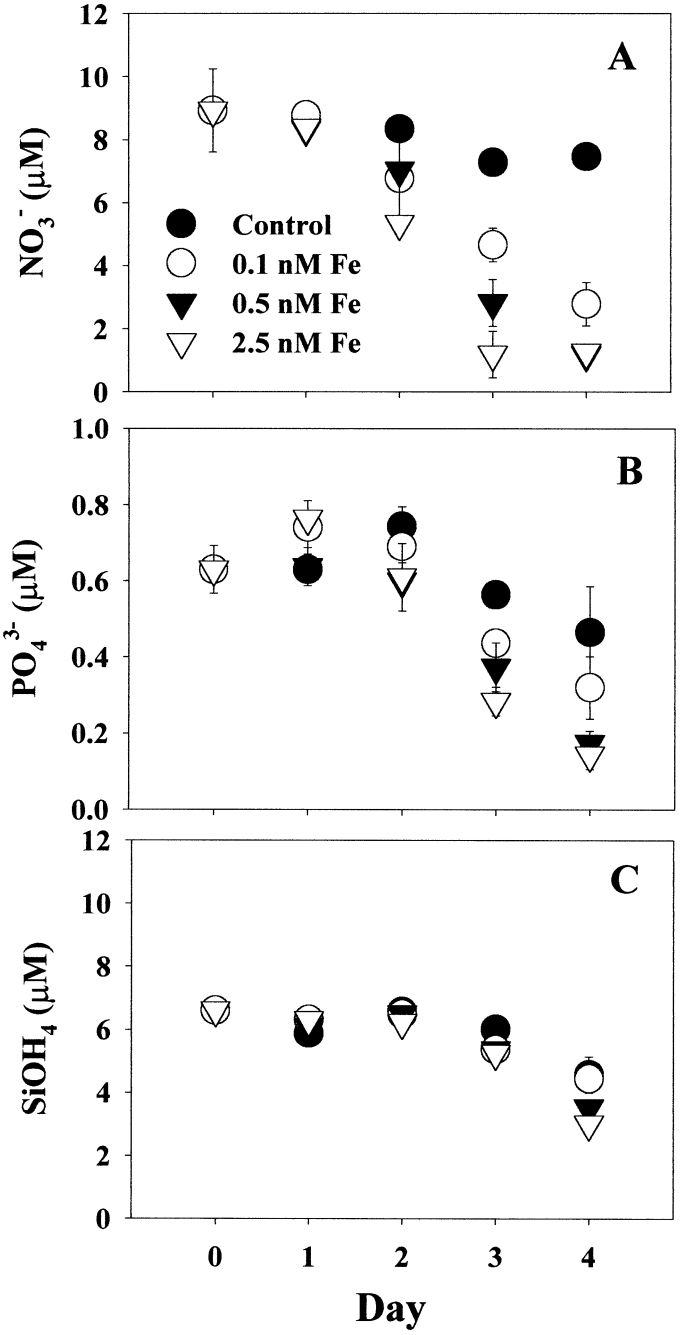

Fig. 5. Major nutrient concentrations during the Humboldt Current experiment. (A) Nitrate. (B) Phosphate. (C) Silicic acid. Symbols and error bars are as in Fig. 2.

mined total Chl *a* (Fig. 7A) in the Peru experiment were broadly similar to those observed in the Humboldt Current. However, the size distribution of community Chl *a* was quite different. Relatively little of the Chl *a* biomass in the Peru incubation was >5 μm (Fig. 7B), ranging from 16% in the initial samples to 16–29% in the day 4 samples (chosen for comparability with the 4-d Humboldt Current incubation). Although large phytoplankton size class Chl *a* did increase slightly in response to the added Fe in the Peru incubations, no major shift toward a large cell-dominated community was seen, and most of the Chl *a* in all treatments throughout the experiment was found in the <5-μm size class.

Initial samples had moderate to high concentrations of the pigments Chl *b*, Chl c_3, 19-but, fucoxanthin, 19-hex, alloxanthin, and zeaxanthin (all >50 ng L^{-1}, Table 1). The high concentration of Chl c_3 and a 19-hex : fucoxanthin ratio of 4.5 indicated dominance by type 3 haptophytes, likely coccolithophorids. Of secondary importance were algae containing Chl *b* (prasinophytes), alloxanthin (cryptophytes), and zeaxanthin (cyanobacteria). The results from the ChemTax analysis confirm these observations (Table 2). Type 3 and type 4 haptophytes and cryptophytes were the most abundant members of this assemblage, and cyanobacteria and prasinophytes were secondary components. Prochlorophytes, pelagophytes, dinoflagellates, chlorophytes, and diatoms were negligible or minor contributors to total community Chl *a*. Total phaeopigments averaged about one-quarter of the total Chl *a* in the initial samples.

Relative changes in HPLC-determined Chl *a* concentrations were similar to fluorometrically determined values (Table 2). Differences in absolute values are due to secondarily fluorescing compounds such as other chlorophylls and chlorophyll degradation products (DiTullio and Geesey 2002). Chl *a* concentration was nearly unchanged in the control bottles but increased to about 3–4× the initial concentration in the Fe addition treatments.

In the control bottles, 19-but and fucoxanthin increased to more than double the initial concentrations while all other pigments decreased or remained the same (Table 1). The 19-hex decreased in the controls but remained fairly constant in the Fe treatments. In +Fe bottles, the greatest increases over initial values were observed for 19-but (3–5×) and fucoxanthin (11–14×). In the Fe addition treatments, Chl *b* concentrations decreased slightly and Chl c_3 concentrations increased slightly compared to the initial values. Alloxanthin and zeaxanthin increased by similar amounts (1–3×). Peridinin increased slightly only in the two highest Fe addition treatments. Phaeopigments increased in all bottles, especially the Fe addition treatments. As a percentage of the total Chl *a* present, though, they were greater in the control than in the four Fe additions.

The ChemTax analyses revealed a more diverse phytoplankton assemblage in the control treatment than in the Fe addition treatments (Table 2). In the control bottles, diatoms were the most abundant group, accounting for slightly less than a third of the Chl *a*, followed by type 3 haptophytes, cryptophytes, pelagophytes, cyanobacteria, and prasinophytes. In the Fe addition treatments, diatoms accounted for over half of the total Chl *a*, with correspondingly less contributions by the other algal groups. All of these treatments, however, are quite different from the initial phytoplankton assemblage.

Flow cytometry results (Fig. 8) also suggested that the response to the added Fe was mostly by eukaryotic phytoplankton, presumably diatoms. Cyanobacterial abundance peaked during the middle of the incubation; although numbers were highest in the 0.8-nM Fe addition, there was no clear stimulation by Fe (Fig. 8A). Eukaryotic nanoplankton exhibited a similar trend (Fig. 8B). Larger eukaryotes were detected as two groups by flow cytometry: a more abundant

Table 4. Dissolved nutrient (NO_3^-, $SiOH_4$, PO_4^{3-}) and particulate (POC, PON, BSi) concentrations from the initial and final days of the Humboldt Current and Peru Upwelling Fe addition experiments and net molar particulate production (BSi : PON, BSi : POC) and dissolved nutrient utilization ($SiOH_4 : NO_3^-$, $NO_3^- : PO_4^{3-}$) ratios during the two experiments. Values are the means and errors are the standard deviations of triplicate bottles.

	Humboldt Current					Peru Upwelling					
			Fe addition (nM)					Fe addition (nM)			
	Initial	Control final	0.1	0.5	2.5	Initial	Control final	0.2	0.4	0.8	2.5
POC (μM)	12.3 ± 2.5	42.6 ± 1.8	44.4 ± 11.2	59.8 ± 11.5	95.7 ± 31.5	9.4 ± 3.9	26.1 ± 4.0	44.8 ± 5.2	60.9 ± 9.5	64.6 ± 13.6	70.4 ± 4.8
PON (μM)	2.0 ± 1.7	5.1 ± 0.0	6.2 ± 0.8	8.2 ± 2.2	13.3 ± 0.6	0.8 ± 0.3	3.2 ± 0.2	7.5 ± 0.7	7.0 ± 1.3	7.0 ± 1.2	8.0 ± 0.8
BSi (μM)	0.3 ± 0.1	2.8 ± 0.9	2.0 ± 0.5	2.7 ± 0.5	2.7 ± 0.6	0.1 ± 0	2.4 ± 0.7	4.4 ± 0.6	5.5 ± 0.3	5.6 ± 0.1	6.3 ± 0.9
BSi : PON produced (mol : mol)	—	0.81	0.40	0.39	0.21	—	0.96	0.64	0.87	0.89	0.86
BSi : POC produced (mol : mol)	—	0.08	0.05	0.05	0.03	—	0.14	0.12	0.10	0.10	0.10
NO_3^- (μM)	8.9 ± 1.3	7.5 ± 0.0	2.8 ± 0.7	1.2 ± 0.1	1.3 ± 0.0	16.3 ± 0.2	8.9 ± 1.7	2.0 ± 1.5	0.2 ± 0.0	0.4 ± 0.1	0.2 ± 0.0
$SiOH_4$ (μM)	5.6 ± 1.0	4.6 ± 0.6	4.5 ± 0.0	3.5 ± 0.1	3.0 ± 0.1	7.8 ± 0.0	6.5 ± 0.6	4.1 ± 1.1	2.6 ± 0.1	2.1 ± 0.2	0.9 ± 0.9
PO_4^{3-} (μM)	0.63 ± 0.06	0.47 ± 0.12	0.32 ± 0.08	0.17 ± 0.13	0.14 ± 0.03	1.2 ± 0.05	0.69 ± 0.11	0.32 ± 1.3	0.13 ± 0.01	0.09 ± 0.03	0.07 ± 0.0
$SiOH_4 : NO_3^-$ used (mol : mol)	—	0.71	0.18	0.27	0.34	—	0.18	0.26	0.32	0.36	0.43
NO_3^- ; PO_4^{3-} used (mol : mol)	—	8.8	19.7	16.7	15.5	—	14.5	16.3	15.0	14.3	14.2

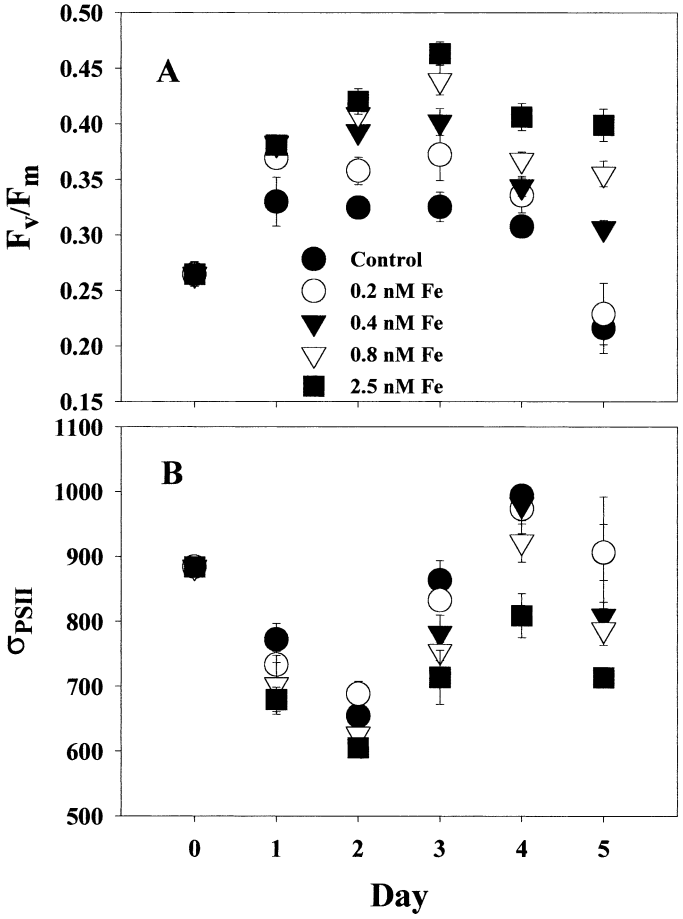

Fig. 6. Photosynthetic parameters in the 5-d Peru Upwelling incubation measured with fast repetition rate fluorometry (FRRF). (A) Photosynthetic efficiency assessed as variable over maximum fluorescence, F_v/F_m. (B) The cross-sectional area of photosystem II, σ_{PSII}. Symbols and error bars represent the means and standard deviations of measurements on triplicate bottles. Controls, closed circles; 0.2-nM Fe additions, open circles; 0.4-nM Fe additions, closed triangles; 0.8-nM Fe additions, open triangles; 2.5-nM Fe additions, closed squares.

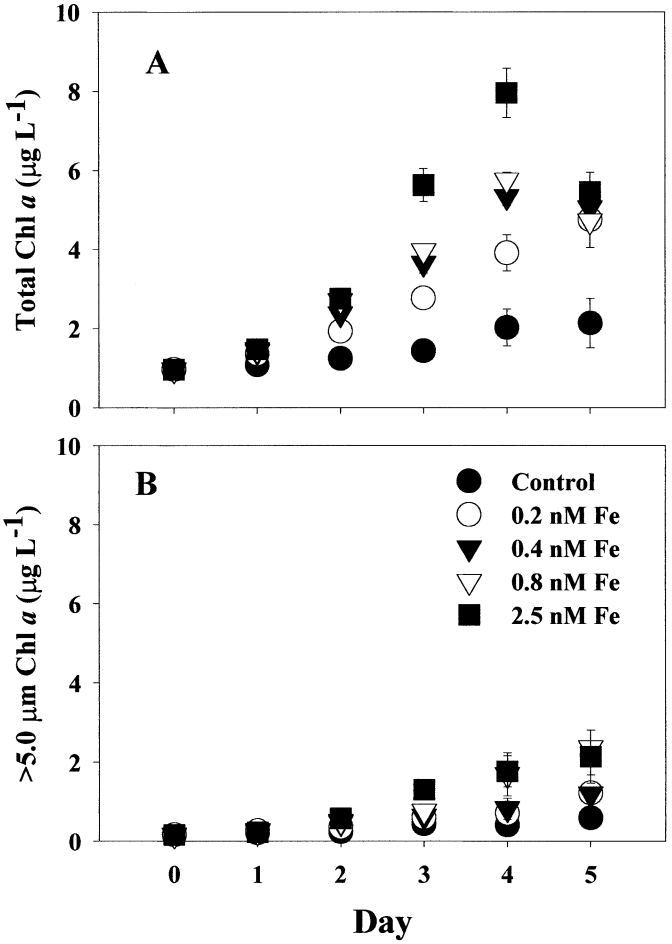

Fig. 7. Fluorometrically determined Chl *a* concentrations in the Peru Upwelling incubations. (A) Total Chl *a*; (B) >5 μm Chl *a*. Symbols and error bars are as in Fig. 6.

group of somewhat smaller cells (Fig. 8C) and a separate group of very large but rare cells (Fig. 8D). Both of these groups increased when Fe was added, although the former grew at all added Fe concentrations, whereas the latter group only increased substantially in the highest (2.5 nM Fe) treatment.

All of the diatoms counted by microscopy were pennates, and most were a single species of small (~1 μm wide, ~10 μm long) unicellular *Nitzschia* (Table 3). Average diatom cell size was much smaller in the Peru samples than in the Humboldt Current incubations, but total cell numbers were an order of magnitude higher, leading to Chl *a* and fucoxanthin levels in the Peru incubations that were comparable to or higher than those in the Humboldt experiment (Tables 1, 2). Final diatom numbers in the 2.5-nM Fe bottles were more than 10× higher than control counts and were at least ~5× higher in the other +Fe samples than in the controls. None of the very large eukaryotes suggested by flow cytometry

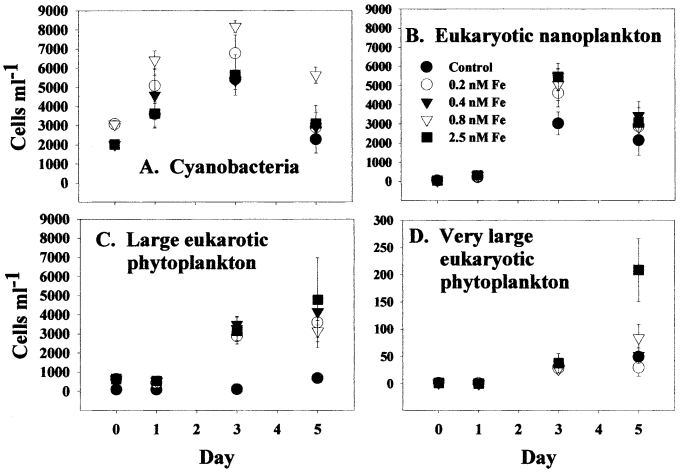

Fig. 8. Results of flow cytometry analyses of phytoplankton abundance during the Peru Upwelling experiment. (A) Cyanobacteria. (B) Eukaryotic nanoplankton. (C) Large eukaryotic phytoplankton, chiefly diatoms. (D) A separate group of very large eukaryotic phytoplankton, likely diatoms. Symbols and error bars are as in Fig. 6.

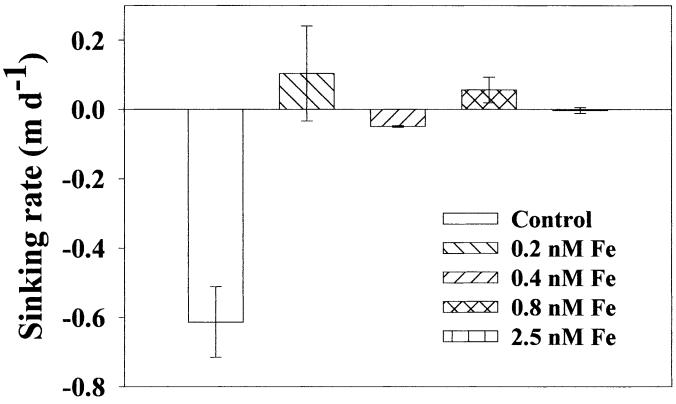

Fig. 9. Sinking rates of the entire phytoplankton community measured on the final day of the Peru Upwelling incubation using the SETCOL method. The horizontal line indicates neutral buoyancy. Values are the means and error bars are the standard deviations of triplicate bottles for each treatment.

were observed, perhaps because they were too rare to detect easily by microscopy. Flagellated *P. globosa* cell numbers increased in three out of the four Fe additions relative to the controls and were higher than in the offshore experiment, but no macroscopic colonies were observed in the Peru incubation. In contrast to the flow cytometry results, visual cell counts also suggested a similar case for nanoflagellates, dinoflagellates, and cyanobacteria. Their abundance was often somewhat higher in +Fe bottles than in controls, although there was large variability among replicates for these groups (Table 3).

Community sinking rates as assessed by the SETCOL method at the end of this incubation were greatly affected by the availability of Fe. Control samples had relatively rapid settling rates of ~0.6 m d^{-1} (Fig. 9). In contrast, phytoplankton in all four of the +Fe treatments were close to neutrally buoyant.

Nutrient biogeochemistry: Nutrient drawdown rates depended on the amount of added Fe, with higher Fe additions resulting in faster utilization. All four treatments with added Fe used most of the original 16.4 μM nitrate by the end of the 5-d incubation (Fig. 10A; Table 4), and the pattern was very similar for phosphate (Fig. 10B). In contrast, control bottles used less than half of the nitrate and phosphate. Unlike the Humboldt Current incubation, increasing Fe additions resulted in progressively greater silicic acid drawdown (Fig. 10C; Table 4).

This effect of Fe on Si drawdown during the Peru incubations was reflected in the net dissolved Si : N drawdown ratios of the community (Table 4). Unlike the previous experiment, Si : N utilization ratios were not highest in the control. Instead, dissolved Si : N drawdown increased with increasing Fe added, although absolute molar utilization ratios were again all quite low (0.18–0.43). Unlike the offshore experiment, net N : P utilization ratios in all control and +Fe treatments were near Redfield values (Table 4).

POC production was incrementally greater as Fe availability increased (Table 4). PON production also increased in the +Fe treatments relative to the controls but was ap-

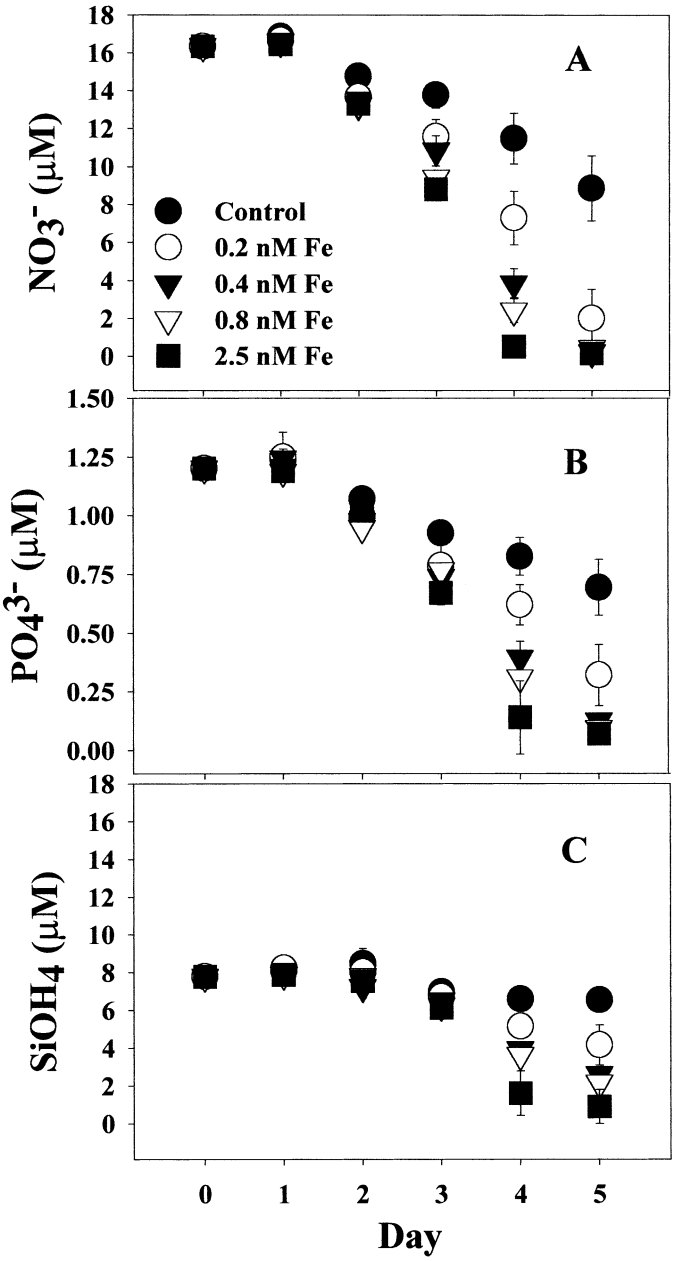

Fig. 10. Major nutrient concentrations during the Peru Upwelling experiment. (A) Nitrate. (B) Phosphate. (C) Silicic acid. Symbols and error bars are as in Fig. 6.

proximately equal at the final timepoint in all +Fe samples. In keeping with the increased silicic acid drawdown at higher Fe levels, BSi production also increased in the same manner. As in the Humboldt Current experiment, BSi : POC production ratios were highest in the controls, but the ratios in the Peru experiment were roughly twice as high. Net BSi : PON production ratios were all much higher (~2–5×) than those calculated from dissolved $Si(OH)_4$ and NO_3^- drawdown and had an opposite trend, with the highest values (0.96) in the controls (Table 4).

Fe concentration versus net specific growth rates—Chl *a* net specific growth rates during the exponential phase of

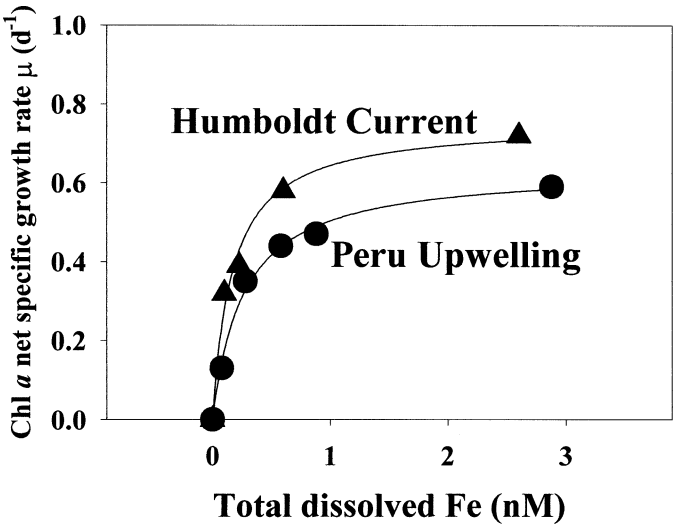

Fig. 11. Chl *a* net specific growth rates (μ) versus total dissolved Fe (nM, added plus ambient) in the Humboldt Current (triangles) and Peru Upwelling (circles) incubations. Curves were forced through the origin by assuming zero growth at a hypothetical zero-Fe concentration. In the Humboldt Current incubation, apparent half-saturation constants for growth were lower ($K_{1/2\ app.}$, 0.17 nM Fe) and apparent maximum net specific growth rates were higher ($\mu_{max\ app.}$, 0.75 d^{-1}) than in the Peru Upwelling community (0.26 nM Fe and 0.64 d^{-1}, respectively). R^2 values for data fitting to the nonlinear saturation curve regressions were 0.86 (Humboldt Current) and 0.99 (Peru Upwelling).

growth in the Humboldt Current and Peru Upwelling incubations could be expressed as saturating functions of total dissolved Fe (ambient plus added) (Fig. 11). In the Humboldt Current incubation, apparent maximum growth rates ($\mu_{max\ app.}$, d^{-1}) were ~1.2× and apparent half-saturation constants for growth ($K_{1/2\ app.}$, nM Fe) were 0.65× those in the Peru Upwelling experiment (Fig. 11). These results suggest that the offshore algal community was able to grow more rapidly at both high (saturating) and low (limiting) concentrations of Fe.

Discussion

Our experiments demonstrate that, as in the California regime, Fe availability can limit primary producers in both the Peru Upwelling and the offshore Humboldt Current. We suggest that the world's largest and most productive coastal upwelling regime is also characterized by widespread Fe-driven HNLC conditions, with all of the consequences for biological productivity and nutrient biogeochemistry that this implies. The South American upwelling regime is likely to be a regional ''mosaic'' of Fe-limited and Fe-replete areas, as is the case along the central California coast (Hutchins et al. 1998).

Peru and California compared—Despite many strong parallels, there are also fundamental physical, biological, and biogeochemical differences between the North and South American upwellings. The ultimate source of Fe in California surface waters is from deposition of continental sediments by wintertime riverine flood runoff, which are then stored on the shelf to supply Fe during the following summer upwelling season (Bruland et al. 2001). This source of Fe is probably not as important in the Peru Upwelling, since it is bordered by the world's driest desert. Peru completely lacks the larger river systems that supply Fe to parts of the California upwelling. Small rivers along the South American west coast do supply snowmelt runoff from the Andes briefly during the austral summer but are essentially dry for most of the year.

Instead, the shallow underlying suboxic waters that are found throughout this region (Morales et al. 1999) may be the major source of Fe to Peruvian surface waters. Fe is highly soluble under low-oxygen conditions (Bruland et al. 1991), and vertical advection and subsequent oxidation of subsurface dissolved Fe(II) during upwelling may supply phytoplankton with much or most of the Fe that supports their growth. In California, upwelled Fe is entrained directly from sediment sources where it has been sequestered after winter flood deposits (Bruland et al. 2001), but in the Peru region, the major biologically available reservoir is likely shelf-derived Fe that has been transported and stored in the suboxic water column. If so, inputs of Fe off Peru may also be less episodic and seasonal than is the case off California.

Upwelling events are also less temporally variable off Peru than in California waters. In coastal California, prevailing winds are favorable for upwelling only during the summer. Even then, the system is characterized by alternating strong upwelling periods followed by extended relaxation events where stratification occurs, allowing phytoplankton to bloom and draw down nutrients (Dugdale and Wilkerson 1989). Because upwelling-derived Fe supplies are curtailed during relaxation, primary producers become much more Fe-limited during these periods (Firme et al. in press).

In contrast, upwelling off Peru occurs to some extent virtually year-round (Minas and Minas 1992), and alternation between strong upwelling events and relaxation conditions is not as commonly observed. The result may be a system in which primary producers do not experience the large fluctuations in Fe availability and limitation effects found over seasonal and shorter time scales off California. However, upwelling intensity in the Peru system is subject to large interannual variability due to effects such as basin-wide El Niño/Southern Oscillation cycles (Codispoti et al. 1982). Changes in upwelled nutrient and Fe supplies undoubtedly affect primary production over longer time scales, just as they do in the equatorial Pacific HNLC area (Barber et al. 1996).

Another major difference between California and Peru is a result of the broader geographical context of the two systems. Ekman-driven upwelling plumes off California are eventually advected into the oligotrophic waters of the California Current, where any residual nutrients they contain are used by the offshore, low-nutrient–adapted, picoplankton-dominated communities typically found here (Bruland et al. 2001). The northwesterly trend of the Humboldt Current off Peru instead feeds more or less directly into the offshore equatorial Divergence. Thus, there is no clearly defined boundary between coastal and oceanic HNLC waters, and

phytoplankton are likely Fe-limited throughout this transitional area, as at our Humboldt Current station.

Phytoplankton community structure—These differences in the physics and chemistry of the two systems are matched by the intriguing differences in phytoplankton community structure we found in our experiments. Unlike California, initial phytoplankton communities in both of the experiments presented here were dominated by haptophytes. Type 4 haptophytes (*P. globosa*) dominated at the offshore station, whereas Type 3 haptophytes (coccolithophorids) were dominant in the Peru Current.

In Fe-limited waters off California, adding Fe virtually always results in massive blooms of large, heavily-silicified diatoms, especially the chain-forming centric genus *Chaetoceros* (Hutchins et al. 1998). In the experiments presented here, Fe additions instead promoted the establishment of a community composed about equally of pennate diatoms and haptophytes. Fe additions allowed diatoms to grow rapidly and become codominant with the haptophytes, whereas the latter responded only slightly or not at all to increased Fe availability. In the Humboldt Current experiment, cryptophytes also benefited greatly from the Fe additions, although they were never dominant.

Surprisingly, it was only at the offshore Humboldt Current station that large diatoms (mostly chain-forming pennates) made a significant contribution to community biomass after Fe addition. This community most closely resembled ones that have been described from the Peruvian shelf region (Rojas de Mendiola 1981; Sellner et al. 1983). In the Peru Upwelling experiment, virtually all of the diatom growth in response to added Fe was by an abundant but very small species of unicellular pennate diatom. Similar small pennate diatom-dominated assemblages have been observed in the past around the Galapagos Islands (Jiminez 1981) and in areas just off the South American shelf (Sellner et al. 1983). The reasons for these differences between Fe effects on diatom community composition in the North and South American ecosystems are unknown, but size structure differences could have large implications for trophic dynamics, nutrient cycles, and, especially, vertical fluxes of elements (Boyd and Newton 1999) in the two regions.

Another novel result was the apparent stimulation of *P. globosa* colony growth by Fe in the Humboldt Current experiment. Type 4 haptophytes (largely *P. globosa* flagellated cells) were prominent in the initial assemblage, but the colonial form was apparently favored by the added Fe. Major nutrient limitation may promote the flagellated form over colonies (Escaravage et al. 1995), and it seems reasonable to suppose that low Fe availabilities might also limit colonial growth because the volume-normalized diffusional Fe flux to a 4-mm-diameter colony is 10^6-fold lower than to a 4-μm flagellated cell at the same external concentration. The importance of *Phaeocystis* in global cycles of elements such as sulfur and their ecological dominance in other regimes such as the Ross Sea, Antarctica (DiTullio et al. 2000; Smith and Asper 2001), makes investigation of these results a priority for future research.

Phytoplankton growth rates as a function of Fe availability—Coale et al. (1996b) plotted Chl *a* growth rates in a number of different equatorial Pacific growout experiments versus Fe concentration in order to estimate Fe half-saturation constants for growth. We used a similar approach, except instead of plotting results from several different incubation experiments begun at different stations, we used growth rate data from the same community incubated at a range of Fe concentrations in each of our two experiments. Differences between the growth responses to Fe availability of the phytoplankton communities are suggested by the saturation curves in Fig. 11. The growth parameters calculated by this type of data analysis should not be interpreted as true physiological constants because the communities are mixed assemblages (not unialgal cultures), and they are not growing at steady state because biomass is increasing and Fe and nutrients are being depleted in batch cultures. Factors other than Fe availability may affect whole-community net maximum specific growth rates. For instance, larger cells (including the bigger diatoms and *Phaeocystis* colonies in our Humboldt Current experiment) may enjoy a degree of immunity to grazing, resulting in higher apparent maximum growth rates.

In spite of these caveats, a saturation curve data treatment such as that presented here yields useful practical information about the potential growth rates of phytoplankton communities following varying levels of Fe inputs. Differences in apparent Fe half-saturation constants for growth ($K_{1/2\ app.}$) are unlikely to be affected by grazing, and should represent actual physiological differences in the whole-community response to Fe availability. In our experiments, the Humboldt Current assemblage had a lower $K_{1/2\ app.}$ (0.17 nM Fe) than the Peru Upwelling community (0.26 nM Fe). This difference suggests that the offshore community was able to grow faster at lower Fe levels, despite a greater degree of dominance by larger diatoms and *Phaeocystis* colonies. Coale et al. (1996b) found a somewhat lower apparent half-saturation constant for growth of 0.12 nM Fe in equatorial Pacific communities, suggesting that oceanic HNLC phytoplankton are more efficient at growing at lower Fe concentrations than either of the communities in our experiments.

Nutrient biogeochemistry and elemental ratios—Molar Si : N utilization ratios in our South American experiments were strikingly lower than in our previous work in the California regime, perhaps because of the differences in phytoplankton communities discussed above. Codominance by nonsiliceous haptophytes and lightly silicified small pennate diatoms likely results in very low utilization of Si relative to N by the phytoplankton community. Similar very low Si : N utilization ratios (~0.2–0.3) have been documented in subantarctic Southern Ocean experiments where the assemblage also was composed of nonsiliceous taxa and very small pennate diatoms (Hutchins et al. 2001). This is in strong contrast to California communities, which are typically dominated by heavily silicified centric diatom species such as *Chaetoceros* (Wilkerson et al. 2000).

Despite low absolute Si : N drawdown ratios in our offshore Humboldt Current experiment, there was still a 2–3× increase under Fe-limited growth conditions in the controls

relative to the Fe-replete treatments. In California, this is not due to increased diatom Si uptake under Fe stress; rather, it results from decreased nitrate assimilation while Si uptake remains relatively constant (Firme et al. in press). However, dissolved Si : N utilization ratios actually increased somewhat with increasing Fe concentrations in the Peru Upwelling incubation. This observation could also be due to species composition differences. Little or no relationship between Si : N drawdown ratios and Fe availability was reported in the nanodiatom- and nanoflagellate-dominated subantarctic experiments mentioned above (Hutchins et al. 2001). It may be that increased Si : N ratios under Fe limitation are a particular feature of communities with large numbers of heavily silicified, large diatom species. Such communities are typically found in California waters and the Southern Ocean south of the Polar Front, where a similar effect was seen for *Fragilariopsis*-dominated communities during SOIREE (Boyd et al. 2000). In regimes where the dominant taxa are unsilicified phytoplankton groups, small lightly silicified pennate diatoms, or both, Si : N drawdown ratios may respond quite differently to changes in Fe levels.

In these experiments, BSi : PON production ratios were much higher than we would have expected from the drawdown ratios of dissolved $Si(OH)_4$ and NO_3^-. These high ratios were not due to discrepancies in silicon uptake and particulate production because mass balance was generally quite good for Si (Table 4). Instead, most of this effect was attributable to the fact that only a portion of the nitrate used was present as PON at the end of the incubations. It is likely that micrograzing was intense in these experiments, judging from the high levels of phaeopigments produced during the incubations and the decreases in small cells like cyanobacteria. The pennate diatoms and nanoflagellates that were abundant in the bottles may have also been small enough to be consumed by large protozoans. We suggest that this may have been an example of the grazer-driven ''silicate pump'' of Dugdale et al. (1995). Much of the nitrate assimilated by grazers may have been converted to ammonium or DON (not measured in our experiments), leaving behind the indigestible BSi. The net result is higher ratios of Si : N in particulate matter than was assimilated by the phytoplankton community. In California, Fe addition experiments are nearly always dominated by very large chain-forming diatoms that are not efficiently grazed in the bottles, and nitrate is usually quantitatively converted to equivalent molar amounts of PON (Hutchins et al. 1998). This may not be the case however in our South American experiments, with their much greater abundances of small phytoplankton species. This suggestion is supported by particulate production ratios that were closer to the dissolved drawdown ratios in the Humboldt Current experiment, with its greater numbers of large phytoplankton, than in the Peru incubation that was almost entirely dominated by small species.

We also saw Fe-driven changes in community N : P utilization ratios in one of our two experiments. N : P drawdown was much lower in Fe-limited controls than in Fe addition treatments, an observation we also made in many other incubation experiments conducted throughout this region (Firme and Hutchins unpubl. data). This suggests that Fe limitation might play an important role in driving non-Redfield behavior of these two nutrients in the South American boundary current system. We suggest that as is the case with changes in Si : N ratios, these shifts in N : P utilization are probably caused by reduced N uptake rather than by increased P assimilation under Fe limitation.

Sinking rates of cultured diatoms and diatom-dominated natural assemblages have previously been shown to be higher during Fe-limited growth (Muggli et al. 1996; Boyd et al. 2000), which should facilitate export of carbon through direct sedimentation of phytoplankton (Smetacek 1985). In our Peru Upwelling experiment, even the lowest added Fe concentration (0.2 nM) was sufficient to change community sinking rates from relatively rapid rates (0.6 m d^{-1}) to near zero. Thus, although phytoplankton carbon fixation is reduced in Fe-limited HNLC regimes, it may be that this carbon is more rapidly transported to underlying waters than in Fe-replete areas.

We conclude that Fe limitation is a major constraint on phytoplankton growth along the South Pacific eastern boundary current, just as it is in the upwelling regime off California. It is now evident that there is a potential for algal Fe limitation anywhere in the ocean where physical processes supply large amounts of major nutrients to surface waters, but where accompanying inputs of Fe are low. Although there are strong similarities in this respect between California and Peru, the two regimes are quite distinct in many other ways. Just as is the case with the three oceanic HNLC areas, these two coastal HNLC areas are very different physical, chemical, and biological environments that share a common limiting nutrient.

References

BARBER, R. T., M. P. SANDERSON, S. T. LINDLEY, F. CHAI, J. NEWTON, D. G. TREES, AND F. P. CHAVEZ. 1996. Primary productivity and its regulation in the equatorial Pacific during and following the 1991–1992 El Niño. Deep-Sea Res. II **43:** 933–970.

BEHRENFELD, M. J., AND P. G. FALKOWSKI. 1999. Widespread Fe limitation of phytoplankton in the South Pacific Ocean. Science **283:** 840–843.

BIENFANG, P. K. 1981. SETCOL: A technologically simple and reliable method for measuring phytoplankton sinking rates. Can. J. Fish. Aquat. Sci. **38:** 1289–1294.

BOYD, P. W., AND OTHERS. 2000. A mesoscale phytoplankton bloom in the polar Southern Ocean stimulated by Fe fertilisation. Nature **407:** 695–702.

———, D. L. MUGGLI, D. E. VARELA, R. H. GOLDBLATT, R. CHRETIEN, K. J. ORIANS, AND P. J. HARRISON. 1996. In vitro Fe enrichment experiments in the NE subarctic Pacific. Mar. Ecol. Prog. Ser. **136:** 179–193.

———, AND P. P. NEWTON. 1999. Does planktonic community structure determine downward particulate organic carbon flux in different oceanic provinces? Deep-Sea Res. I **46:** 63–91.

BRULAND, K. W., J. R. DONAT, AND D. A. HUTCHINS. 1991. Interactive influences of bioactive trace metals on biological production in oceanic waters. Limnol. Oceanogr. **36:** 1555–1577.

———, E. L. RUE, AND G. J. SMITH. 2001. Fe and macronutrients in California coastal upwelling regimes: Implications for diatom blooms. Limnol. Oceanogr. **46:** 1661–1674.

BRINK, K. H., AND OTHERS. 1995. Group report: How do coastal upwelling systems operate as integrated physical, chemical, and biological systems and influence the geological record?

The role of physical processes in defining the spatial structures of biological and chemical variables, p. 103–124. *In* C. P. Summerhayes et al. [eds.], Upwelling in the ocean: Modern processes and ancient records. Wiley.

BRZEZINSKI, M. A. 1985. The Si:C:N ratio of marine diatoms: Interspecific variability and the effect of some environmental variables. J. Phycol. **21:** 347–357.

———, AND D. M. NELSON. 1995. The annual silica cycle in the Sargasso Sea near Bermuda. Deep-Sea Res. I **42:** 1215–1237.

CHAVEZ, F. P., AND J. R. TOGGWEILER. 1995. Physical estimates of global new production: The upwelling contribution, p. 313–320. *In* C. P. Summerhayes et al. [eds.], Upwelling in the ocean: Modern processes and ancient records. Wiley.

COALE, K. H., AND OTHERS. 1996*a*. A massive phytoplankton bloom induced by an ecosystem-scale Fe fertilization experiment in the equatorial Pacific Ocean. Nature **383:** 495–501.

———, S. E. FITZWATER, R. M. GORDON, K. S. JOHNSON, AND R. T. BARBER. 1996*b*. Control of community growth and export production by upwelled Fe in the equatorial Pacific. Nature **379:** 621–624.

CODISPOTI, L. A., R. C. DUGDALE, AND H. J. MINAS. 1982. A comparison of the nutrient regimes off northwest Africa, Peru and Baja California. Rapp. P.-v. Reun. Cons. Int. Explor. Mer **180:** 184–201.

DE BAAR, H. J. W., A. G. J. BUMA, R. F. NOLTING, G. C. CADEE, G. JACQUES, AND P. J. TREGUER. 1990. On Fe limitation of the Southern Ocean: Experimental observations in the Weddell and Scotia Seas. Mar. Ecol. Prog. Ser. **65:** 105–122.

DITULLIO, G. R., D. A. HUTCHINS, AND K. W. BRULAND. 1993. Interaction of Fe and major nutrients controls phytoplankton growth and species composition in the tropical north Pacific Ocean. Limnol. Oceanogr. **38:** 495–506.

———, AND OTHERS. 2000. Rapid and early export of *Phaeocystis antarctica* blooms in the Ross Sea, Antarctica. Nature **404:** 595–598.

———, AND M. E. GEESEY. 2002. Photosynthetic pigments in marine algae and bacteria, p. 2453–2470. *In* G. Bitton [ed.], Encyclopedia of environmental microbiology, vol. 5. Wiley.

———, ———, A. LEVENTER, AND M. P. LIZOTTE. In press. Algal pigment ratios in the Ross Sea: Implications for ChemTax analysis of Southern Ocean data. *In* G. R. DiTullio and R. B. Dunbar [eds.], Biogeochemistry of the Ross Sea. AGU Antarctic Research Series.

DUGDALE, R. C., AND F. P. WILKERSON. 1989. New production in the upwelling center at Point Conception, California: Temporal and spatial patterns. Deep-Sea Res. **36:** 985–1007.

———, ———, AND H. J. MINAS. 1995. The role of a silicate pump in driving new production. Deep-Sea Res. I **42:** 697–719.

DURAND, M. D., AND R. J. OLSON. 1996. Contributions of phytoplankton light scattering and cell concentration changes to diel variations in beam attenuation in the equatorial Pacific from flow-cytometric measurements of pico-, ultra-, and nanoplankton. Deep-Sea Res. II **43:** 891–906.

ESCARAVAGE, V., L. PEPERZAK, T. C. PRINS, J. C. PETERS, AND J. C. JOORDENS. 1995. The development of a *Phaeocystis* bloom in a mesocosm experiment in relation to nutrients, irradiance and coexisting algae. Ophelia **42:** 55–74.

FALKOWSKI, P. G., AND Z. KOLBER. 1995. Variations in chlorophyll fluorescence yields in phytoplankton in the world's oceans. Aust. J. Plant Physiol. **22:** 341–355.

FIRME, G. F., K. W. BRULAND, E. L. RUE, D. A. WEEKS, AND D. A. HUTCHINS. In press. Spatial and temporal variability in phytoplankton iron limitation along the California coast and consequences for Si, N and C biogeochemistry. Global Biogeochemical Cycles.

GIESKES, W. W., AND G. W. KRAAY. 1983. Dominance of Cryptophyceae during the phytoplankton spring bloom in the Central North Sea detected by HPLC analysis of pigments. Mar. Biol. **75:** 179–185.

HUTCHINS, D. A., AND K. W. BRULAND. 1998. Fe-limited diatom growth and Si:N uptake ratios in a coastal upwelling regime. Nature **393:** 561–564.

———, G. R. DITULLIO, Y. ZHANG, AND K. W. BRULAND. 1998. An Fe limitation mosaic in the California upwelling regime. Limnol. Oceanogr. **43:** 1037–1054.

———, P. N. SEDWICK, G. R. DITULLIO, P. W. BOYD, B. GRIFFITHS, B. QUEGUINER, AND C. CROSSLEY. 2001. Fe and silicic acid limitation of phytoplankton growth in the subantarctic Southern Ocean: Experimental results from the SAZ project. J. Geophys. Res., C **106:** 31,559–31,572.

JIMINEZ, R. 1981. Composition and distribution of phytoplankton in the upwelling system of the Galapagos Islands, p. 327–338. *In* F. A. Richards [ed.], Coastal upwelling, coastal and estuarine sciences 1. American Geophysical Union.

JOHNSON, K. S., F. P. CHAVEZ, AND G. E. FRIEDERICH. 1999. Continental-shelf sediment as a primary source of Fe for coastal phytoplankton. Nature **398:** 697–700.

MACKEY, M. D., D. J. MACKEY, H. W. HIGGINS, AND S. W. WRIGHT. 1996. CHEMTAX—a program for estimating class abundances from chemical markers: Application to HPLC measurements of phytoplankton. Mar. Ecol. Prog. Ser. **144:** 265–283.

MARTIN, J. H., AND OTHERS. 1994. Testing the iron hypothesis in ecosystems of the equatorial Pacific Ocean. Nature **371:** 123–129.

———, R. M. GORDON, AND S. E. FITZWATER. 1991. The case for Fe. Limnol. Oceanogr. **36:** 1793–1802.

MINAS, H. J., AND M. MINAS. 1992. Net community production in ''High Nutrient–Low Chlorophyll'' waters of the tropical and Antarctic Oceans: Grazing versus Fe hypothesis. Oceanologica Acta **15:** 145–162.

MORALES, C. E., S. E. HORMAZABAL, AND J. L. BLANCO. 1999. Interannual variability in the mesoscale distribution of the depth of the upper boundary of the oxygen minimum layer off northern Chile (18–24S): Implications for the pelagic system and biogeochemical cycling. J. Mar. Res. **57:** 909–932.

MUGGLI, D. L., M. LECOURT, AND P. J. HARRISON. 1996. Effects of Fe and nitrogen source on the sinking rate, physiology and metal composition of an oceanic diatom from the subarctic Pacific. Mar. Ecol. Prog. Ser. **132:** 215–227.

ROJAS DE MENDIOLA, B. 1981. Seasonal phytoplankton distribution along the Peruvian coast, p. 348–356. *In* F. A. Richards [ed.], Coastal upwelling, coastal and estuarine sciences 1. American Geophysical Union.

RUE, E. L., AND K. W. BRULAND. 1997. The role of organic complexation on ambient Fe chemistry in the equatorial Pacific Ocean and the response of a mesoscale Fe addition experiment. Limnol. Oceanogr. **42:** 901–910.

RUETER, J. G., D. A. HUTCHINS, R. W. SMITH, AND N. L. UNSWORTH. 1992. Fe nutrition of *Trichodesmium*, p. 289–306. *In* E. J. Carpenter, D. G. Capone, and J. G. Rueter [eds.], Marine pelagic cyanobacteria: *Trichodesmium* and other diazotrophs. Kluwer.

RYTHER, J. H. 1969. Photosynthesis and fish production in the sea. Science **166:** 72.

SELLNER, K. G., P. HENDRIKSON, AND N. OCHOA. 1983. Relationship between the chemical composition of particulate organic matter and phytoplankton distributions in recently upwelled waters of Peru, p. 273–288. *In* E. Suess and J. Theide [eds.], Coastal upwelling its sediment record. Part A: Responses of

the sedimentary regime to persistent coastal upwelling. Plenum.

SMETACEK, V. S. 1985. Role of sinking in diatom life-history cycles—ecological, evolutionary and geological significance. Mar. Biol. **84:** 239–251.

SMITH, W. O., AND V. A. ASPER. 2001. The influence of phytoplankton assemblage composition on biogeochemical characteristics and cycles in the southern Ross Sea, Antarctica. Deep-Sea Res. I **48:** 137–161.

WELSCHMEYER, N. A. 1994. Fluorometric analysis of chlorophyll *a* in the presence of chlorophyll *b* and pheopigments. Limnol. Oceanogr. **39:** 1985–1992.

WILKERSON, F. P., R. C. DUGDALE, R. M. KUDELA, AND F. P. CHAVEZ. 2000. Biomass and productivity in Monterey Bay, California: Contribution of large phytoplankton. Deep-Sea Res. II **47:** 1003–1022.

Received: 10 October 2001
Accepted: 29 January 2002
Amended: 13 March 2002